Fast Nuclear Spin Hyperpolarization of Phosphorus in Silicon

D. R. McCamey,[1,*] J. van Tol,[2] G. W. Morley,[3] and C. Boehme[1,†]

[1]*Department of Physics, University of Utah, 115 South 1400 East Rm 201, Salt Lake City, Utah 84112, USA*
[2]*Center for Interdisciplinary Magnetic Resonance, National High Magnetic Field Laboratory at Florida State University,*
Tallahassee, Florida 32310, USA
[3]*London Centre for Nanotechnology and Department of Physics and Astronomy, University College London,*
London WC1H 0AH, United Kingdom

We experimentally demonstrate a method for obtaining nuclear spin hyperpolarization, that is, polarization significantly in excess of that expected at thermal equilibrium. By exploiting a nonequilibrium Overhauser process, driven by white light irradiation, we obtain more than 68% negative nuclear polarization of phosphorus donors in silicon. This polarization is reached with a time constant of ~ 150 sec, at a temperature of 1.37 K and a magnetic field of 8.5 T. The ability to obtain such large polarizations is discussed with regards to its significance for quantum information processing and magnetic resonance imaging.

Phosphorus doped crystalline silicon (Si:P) is a model system for investigating spin effects in the solid state and at the same time is a point defect with great technological importance. Si:P has been used since the beginning of the semiconductor industry in the early 1950's for applications ranging from the ubiquitous (thin film transistors) to the conceptual (single electron transistors). The ability to hyperpolarize the spins in this material is important for a number of its applications. Utilizing the nuclear spin of phosphorus donors as quantum bits [1,2] relies on the ability to obtain a well characterized initial state [3], which can be obtained by hyperpolarization. Spin polarized silicon microparticles may also have applications for magnetic resonance imaging techniques [4], similar to other hyperpolarized systems, such as xenon [5]. While it is reasonably simple to obtain large electron spin polarization, for example, by using moderate magnetic fields at liquid ⁴He temperatures, doing the same with nuclear spins is difficult due to their much smaller Zeeman splitting. There are a number of schemes used to obtain nuclear spin polarization in excess of the thermal polarization. Dynamic nuclear polarization using off-resonance radiation has been studied extensively [4,6]. Complex pulses or adiabatic passage effects may be used to manipulate spin states, leading to large polarizations [7,8]. Electrical injection of hot carriers has been used to obtain positive polarizations [9]; however, this requires electrical contact to the sample. Optical excitation with linearly polarized sub band gap light has given small ($\sim 0.25\%$) polarization of ²⁹Si nuclei in silicon with a natural isotopic abundance [10]. Other materials, such as GaAs, have demonstrated nuclear spin polarization over 25% following pumping with polarized light [11], although we note that these materials are not biologically compatible.

In this Letter, we demonstrate negative polarization of phosphorus donor nuclei in silicon of up to $P = -68\%$.

The scheme used is simple, fast and does not involve resonant manipulation of either the nuclear or electronic spin. Instead, the relative populations are modified using photoexcited carriers, generated using white light, at low temperatures (about ⁴He temperature) and in magnetic fields (~ 8.5 T) significantly smaller than those required to obtain an equivalent thermal nuclear spin polarization.

Phosphorus (³¹P) in Si consists of a spin-1/2 donor electron coupled to a spin-1/2 nucleus. This provides a system with four energy levels (Fig. 1) in presence of strong magnetic fields. At $B_0 \approx 8.5$ T, the donor electron
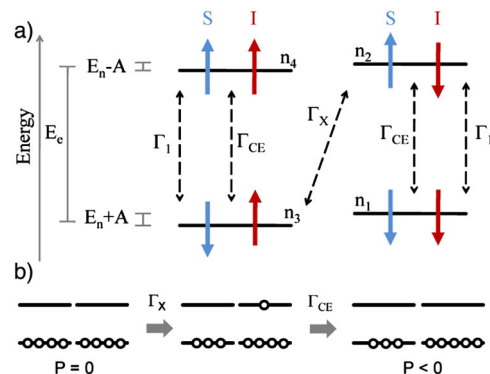

FIG. 1 (color online). (a) Sketch of the energy levels of the four spin eigenstates of a phosphorus donor atom in silicon in presence of very high magnetic fields. The dashed arrows indicate allowed transitions with their respective rate coefficients. Γ_1 is for longitudinal relaxation processes, Γ_{CE} for relaxation driven by capture-emission of conduction electrons and Γ_X for the Overhauser flip-flop process. The two different nuclear orientations are offset horizontally. (b) Simplified sketch of the change from a thermally polarized spin ensemble to a hyperpolarized spin ensemble using $T_p > T_e$, to illustrate qualitatively the polarization process. Note that the spin relaxation processes act continuously (not sequentially as illustrated).

Zeeman splitting $\Delta E_e \approx 240$ GHz, the nuclear Zeeman energy $\Delta E_n \approx 147$ MHz and the hyperfine interaction $A = 117$ MHz.

Figure 1(a) shows the relevant spin relaxation processes that occur in the ^{31}P donor system. The population in each of the four possible spin configurations are labeled n_1 through n_4. Γ_1 is the rate coefficient associated with longitudinal relaxation of the electron magnetization towards thermal equilibrium with the lattice phonons at temperature T_p. Γ_X is the rate coefficient associated with the Overhauser spin relaxation process (a flip-flop) between the electron and nuclear spins [12]. The Overhauser rate $T_X \propto B_0^{-2}T_p^{-1}$ (Ref. [13]) where B is the applied magnetic field. The transition between n_1 and n_4 is forbidden.

Both the Overhauser (Γ_X) and longitudinal-Γ_1 spin relaxation are dominated by phonon mediated processes. There are two sources of phonons in this system. The first is the equilibrium phonon distribution generated by the helium bath in which the silicon is placed. When we shine light onto the sample, however, we generate hot photocarriers high in the conduction band. As these hot photocarriers equilibrate they emit phonons, which are in addition to the equilibrium phonons in the material. We capture the resulting nonequilibrium phonon distrubution by introducing a quasitemperature, T_p, which characterizes the spin population distribution the phonons generate via both the Γ_X and Γ_1 processes.

In contrast to spin relaxation in silicon in the dark, an additional longitudinal relaxation mechanism exists which is driven by the photoexcited electrons. The photoexcited electrons can be captured by a phosphorus donor [14] forming a charged state, with subsequent emission of the extra electron leading to spin relaxation [15]. We capture this in our rate picture by introducing Γ_{CE}. This capture-emission process may be the dominant spin relaxation mechanism of donor electrons [15], resulting in the donor spins assuming the temperature of the thermalized photocarriers, T_e. The electrons which contribute to this process are almost exclusively the thermalized electrons, as the thermalization time is much shorter than the carrier lifetime.

We point out that the temperature that characterizes the spin distribution of the thermalized carriers in semiconductors, T_e, is not necessarily the same as T_p [16]. In Si:P, this leads to a situation where the dominant mechanism for Overhauser relaxation (Γ_X) is attempting to move the spin system to a different temperature (T_p) than the dominant mechanism for electron spin relaxation (Γ_{CE}, T_e). We note that differences between T_p and T_e have previously been demonstrated using electrical injection of hot carriers [17].

Feher has previously discussed the effect of the phonon temperature on the polarization of phosphorus in silicon [17]. He has shown that, if the two characteristic temperatures of our system are unequal, $T_p \neq T_e$, then the thermally (hardly) polarized equilibrium population distribution is modified. The Overhauser process will try to

achieve thermal equilibrium between states n_2 and n_3 at a temperature T_p, and the capture-emission spin relaxation process will force states (n_1 and n_2) and (n_3 and n_4) to thermal equilibrium at temperature T_e. Figure 1(b) illustrates this process. For $T_p > T_e$, this leads to the population of n_1 becoming much larger than the population of all other states, resulting in a net negative nuclear polarization, since $P = \frac{(n_3+n_4)-(n_1+n_2)}{(n_1+n_2)+(n_3+n_4)}$. Conversely, $T_e > T_p$ results in nuclear polarization. We note that spin relaxation of conduction electrons is extremely fast, indicating negligible conduction electron mediated spin interaction between donors.

To investigate this effect, we have undertaken electron spin resonance (ESR) and electrically detected magnetic resonance (EDMR) experiments at $B \approx 8.5$ T, corresponding to a resonant frequency, $f = 240$ GHz [18,19]. Similar experiments have been described by us elsewhere [15,20]. The samples used in this study were similar to those described in Ref. [20]. They consist of crystalline Si (111) with a phosphorus doping density $[P] \sim 10^{15}$ cm^{-3}, with aluminum surface contacts to allow EDMR.

Figure 2(a) shows two ESR spectra recorded at $B \approx$ 8.5 T and $T = 3$ K by sweeping B_0. We fit the two observed resonances with two Gaussian line shapes. We can be sure the signal is from phosphorus donor electrons due to both the g-factor and hyperfine splitting of 4.17 mT. The low-field [high-field] resonance is due to nuclear spins aligned ($\uparrow$) [antialigned ($\downarrow$)] with the external field. The resonances are saturated due to the long relaxation times; however, we assume that the relaxation times are the same and, as a result, can take the area of the resonance as a measure of the number of spins that contribute to it [8]. We
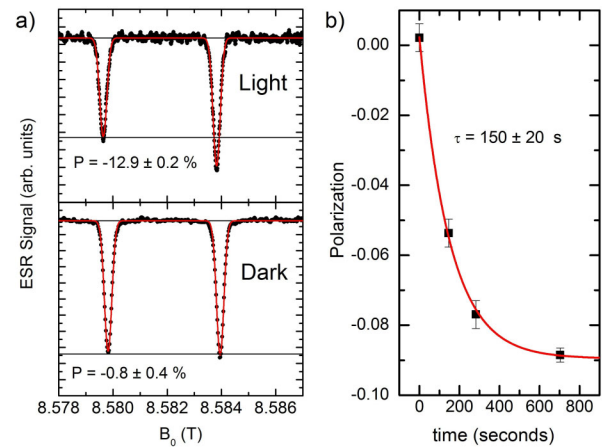

FIG. 2 (color online). (a) ESR spectra, measured at $T = 3$ K with $f_{res} = 240$ GHz, with (top) and without (bottom) illumination by a mercury discharge lamp. The polarization is determined by comparing the areas of the two resonances, obtained by fitting the data with two Gaussian line shapes separated by the phosphorus hyperfine splitting, $\Delta B = 4.17$ mT (solid line). (b) The ^{31}P nuclear polarization obtained from EPR spectra, measured as a function of illumination time, at $T = 3$ K. The solid line is a single exponential fit to the data.

thus determine the polarization of the sample, $P = \frac{(\uparrow - \downarrow)}{(\uparrow + \downarrow)}$.
The lower spectrum was recorded in the dark, and shows a
nuclear polarization $P = -0.008 \pm 0.004$. Next, light
from a mercury discharge lamp was shone onto the top
side of the sample through an optical fiber, and the ESR
spectrum was remeasured (upper spectrum). Again, two
resonances are visible; however, they have different inten-
sities. Here, we determine the nuclear spin polarization
$P = -0.129 \pm 0.002$. This is a change in polarization over
the expected thermal polarization by a factor $\eta = P/P_0 \approx$
-78. A similar result is obtained sweeping B_0 in the
opposite direction, indicating that the polarization is not
a passage effect [13].

The polarization model discussed above predicts that the
time taken to reach a steady-state polarization should be
limited by the Overhauser rate, since $1/T_X = \Gamma_X \ll \Gamma_1$,
Γ_{CE}. By using previously measured [21] low magnetic field
($B \approx 340$ mT) values for T_X, and extrapolating to the field
used in the experiments presented here using the relation-
ship of Pines *et al.* [13], we obtain for the Overhauser time
$T_X \approx 65$ s, for $T_p = 3$ K and $B_0 = 8.5$ T. Figure 2(b)
shows the polarization measured via ESR after light was
applied to the sample. The data show a gradual approach to
a nonequilibrium steady state. The fit of these data with a
single exponential decay function shows excellent agree-
ment and yields a time constant of $\tau = 150 \pm 20$ s. We
believe this is in very good agreement with predictions of
the Overhauser rate [13], given the uncertainty of the low-
field value (~ 30 h), and the extrapolation over nearly
2 orders of magnitude of the magnetic field on which the
Overhauser rate depends quadratically.

One aspect of the experiment above suggests that the
polarization measured with ESR is a lower limit on the
maximum polarization obtained. ESR measures the polar-
ization in the entire sample; however, only the surface is
illuminated. We expect that, while the charge carriers will
diffuse throughout the sample, they will thermalize much
faster than they can diffuse. This will lead to a strong depth
inhomogeneity of the phonon temperature and hence a
depth dependence of the polarization. The polarization
will be largest near the surface which is being illuminated
and smallest on the opposite surface.

EDMR is a magnetic resonance detection scheme which
is sensitive to spins close to the illuminated surface. EDMR
relies on the current through a sample being influenced by
the observed spin state. In Si:P at high magnetic fields, we
have shown [15] that EDMR is observed due to the spin
dependent capture-emission mechanism described by
Thornton and Honig [22], which we have included in our
polarization model as Γ_{CE}. This process decreases the
current through the sample when donor electrons are res-
onantly excited. To measure EDMR, we thus require free
charge carriers, which are provided by the illumination
used to polarize the nuclear spins. Figure 3(a) shows an
EDMR spectrum recorded at $T = 1.37$ K, the lowest tem-
perature accessible to us. The spectrum was measured

during xenon discharge lamp illumination [23], and with
a current, $I_{SD} = 500$ nA. The microwaves were chopped at
a frequency of 908 Hz, and the change in current recorded
with a lock-in amplifier. As with the ESR measurements,
the spectrum is well fit by two Gaussian line shapes sepa-
rated by the hyperfine splitting. Again, we use the area of
the resonances as a measure of the population in each
nuclear spin state. The polarization measured here is $P =$
$-68 \pm 1\%$. This corresponds to an enhancement over the
equilibrium polarization of $\eta \approx 190$, and to an effective
nuclear spin temperature of ≈ -5 mK.

We have used EDMR to test some qualitative properties
of the polarization model, namely, the dependence of the
nuclear polarization on lattice temperature and illumina-
tion intensity. Figure 3(b) shows the ^{31}P polarization in-
creasing monotonically with decreasing lattice tempera-
ture below $T \approx 3$ K. Based on the rate model presented in
Fig. 1, we calculated the polarization using the measured
bath temperature as T_e and a constant phonon temperature
whose value was chosen to fit the experimental data. The
simulation results are also shown in Fig. 3(b). The best fit
of the simulated values to the measured values was
achieved for $T_p = 2.7$ K, in agreement with the expecta-
tion that hyperpolarization vanishes when $T_e \approx T_p$. We also
found that the ratio $\Gamma_{CE}/\Gamma_1 \approx 4$, in reasonable agreement
with our previous work [15]. Note that there is significant
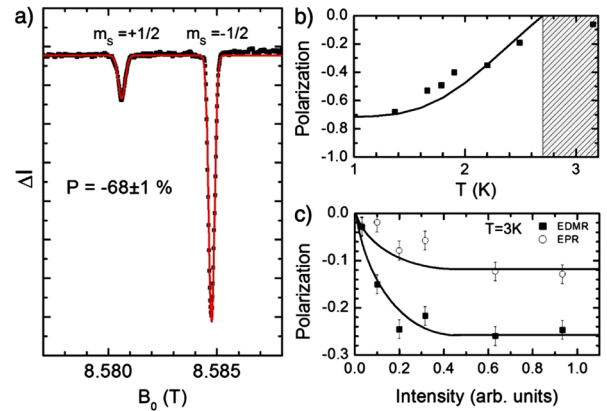discrepancy for temperatures above $T_e = 2.5$ K. While the

FIG. 3 (color online). (a) Electrically detected magnetic reso-
nance spectrum of Si:P at $T = 1.37$ K under illumination. The
spectrum was fit with two Gaussian line shapes, and the nuclear
polarization determined by comparing the area of the hyperfine
split resonances. Here, $P = -68 \pm 1\%$. (b) The polarization
determined from EDMR measurements for a number of different
temperatures. The line is a numerical simulation of the expected
polarization using the rate model presented in this Letter. The
shaded region indicates where our model does not hold. See text
for details. The measurements in (a) and (b) were obtained using
a xenon discharge lamp. (c) The polarization measured simul-
taneously with ESR and EDMR, as a function of the illumination
intensity of the mercury discharge lamp used to generate the
photocarriers, measured at $T = 3$ K. The lines are guides to the
eye, and are scaled by a factor of approximately 2.5 between the
ESR and the EDMR.

calculated data predicts no polarization, the measured data shows a clear hyperpolarization of $P = -6\%$ at 3 K. We attribute this discrepancy to our assumption of a constant T_p used in the calculation. Note that the negative polarization we observe implies $T_p > T_e$. Hence, the assumption of a constant $T_p = 2.7$ K used for these simulations becomes unrealistic at $T_e > 2.7$ K. Far above 2.7 K, we anticipate that $T_e = T_p$, and thus no polarization should occur.

In order to further test the polarization model we changed the excitation spectrum of the excess charge carriers from the xenon lamp used for the acquisition of the data in Fig. 3(a) and 3(b) to a mercury lamp which has a higher spectral temperature [24]. For the latter we measured polarization with both EDMR and ESR at a constant bath temperature of $T = 3$ K. As shown in Fig. 3(c), the EDMR spectra recorded with the mercury lamp yield a significantly higher polarization of up to $P = -24\%$ (instead of -6% at $T = 3$ K), independently of the intensity over a range of almost 1 order of magnitude. As expected, at low intensities, when the excess charge carrier densities drop into a range where the longitudinal relaxation is dominated by the phonon process, the nuclear polarization vanishes and equilibrium appears. The polarization measured with ESR was consistently $\approx 45\%$ of that measured with EDMR, agreeing with our hypothesis that T_p is inhomogeneous throughout the sample.

Note that while we have demonstrated polarization above $P = -68\%$, our model predicts the possibility of even higher negative polarization at lower temperatures and higher optical excitation rates. Numerical modeling of this process with the realistic values $T_e = 1$ K and $T_p = 3$ K, and with $\Gamma_{CE} \gg \Gamma_1 \gg \Gamma_X$, indicate that negative polarization over 95% is achievable. The technical simplicity of this polarization method suggests that it may be beneficial for a variety of applications. For instance, silicon microparticles are biologically inert which makes them prime candidates as contrast agents for *in vivo* magnetic resonance imaging. We see no obvious reason why the polarization technique presented above will not provide the same level of polarization in microparticles as we have demonstrated in bulk material. Given room temperature spin lifetimes >20 min for ^{31}P nuclei in amorphous silicon, a disordered material with a bigger defect density and a larger hyperfine interaction than crystalline silicon, we expect polarization lifetimes of over an hour for this material, easily allowing implementation of such experiments [25]. However, further investigation of the ability to polarize material with higher ^{31}P density must be undertaken to determine the feasibility of this material as an imaging agent. Rapid polarization of ^{31}P nuclear spins demonstrated may also offer an initialization mechanism for ^{31}P in silicon spin qubits.

In conclusion, we have experimentally demonstrated negative hyperpolarization ($>68\%$) of phosphorous donor nuclear spins in crystalline silicon. The polarization is due to irradiation with above band gap light, at low temperatures and high magnetic fields. The process is driven by the Overhauser effect, leading to fast polarization times (of order minutes). We hypothesize a model for the physical process which leads to this polarization based on different phonon and electron temperatures, and show that the qualitative predictions of this model for the polarization dependence on the bath temperature, illumination temperature, and intensity show reasonable agreement to the experimental data.

*dane.mccamey@physics.utah.edu
†boehme@physics.utah.edu

[1] B. E. Kane, Nature (London) **393**, 133 (1998).
[2] J. J. L. Morton *et al.*, Nature (London) **455**, 1085 (2008).
[3] D. P. DiVincenzo, Fortschr. Phys. **48**, 771 (2000).
[4] A. E. Dementyev, D. G. Cory, and C. Ramanathan, Phys. Rev. Lett. **100**, 127601 (2008).
[5] L. Schroder *et al.*, Science **314**, 446 (2006).
[6] A. Abragam and M. Goldman, Rep. Prog. Phys. **41**, 395 (1978).
[7] G. Feher and E. A. Gere, Phys. Rev. **103**, 501 (1956).
[8] G. W. Morley *et al.*, Phys. Rev. Lett. **98**, 220501 (2007).
[9] W. G. Clark and G. Feher, Phys. Rev. Lett. **10**, 134 (1963).
[10] A. S. Verhulst *et al.*, Phys. Rev. B **71**, 235206 (2005).
[11] S. E. Hayes, S. Mui, and K. Ramaswamy, J. Chem. Phys. **128**, 052203 (2008).
[12] A. W. Overhauser, Phys. Rev. **92**, 411 (1953).
[13] D. Pines, J. Bardeen, and C. P. Slichter, Phys. Rev. **106**, 489 (1957).
[14] A. Honig and M. Moroz, Rev. Sci. Instrum. **49**, 183 (1978).
[15] G. W. Morley *et al.*, Phys. Rev. Lett. **101**, 207602 (2008).
[16] S. A. Lyon, J. Lumin. **35**, 121 (1986).
[17] G. Feher, Phys. Rev. Lett. **3**, 135 (1959).
[18] J. van Tol, L.-C. Brunel, and R. J. Wylde, Rev. Sci. Instrum. **76**, 074101 (2005).
[19] G. W. Morley, L.-C. Brunel, and J. van Tol, Rev. Sci. Instrum. **79**, 064703 (2008).
[20] D. R. McCamey *et al.*, Phys. Rev. B **78**, 045303 (2008).
[21] G. Feher and E. A. Gere, Phys. Rev. **114**, 1245 (1959).
[22] D. D. Thornton and A. Honig, Phys. Rev. Lett. **30**, 909 (1973).
[23] Xenon Lamp: Irradiance ≈ 20 mW/cm^2, Power ≈ 1 mW, approximately Gaussian spectrum with a central wavelength $\lambda_c \approx 570$ nm and width $\Delta\lambda_w \approx 220$ nm.
[24] Mercury Lamp: Irradiance ≈ 150 mW/cm^2, Power ≈ 7.5 mW, more discrete, emission line spectra.
[25] M. J. McCarthy and J. A. Reimer, Phys. Rev. B **36**, 4525 (1987).